

# On the role of grain-boundary migration during the creep of zinc

VAKIL SINGH, P. RAMA RAO

*Department of Metallurgical Engineering, Banaras Hindu University, Varanasi, India*

D. M. R. TAPLIN

*Department of Mechanical Engineering, University of Waterloo, Waterloo, Ontario, Canada*

Constant engineering strain-rate tensile tests have been carried out in the temperature range 20 to 150°C on high purity Zn, Zn-0.14 at. % Cu (alloy C) and Zn-0.16 at. % Al (alloy A) alloys. Measurements of angular distribution of orientations of grain boundaries have been used to study grain-boundary migration during deformation. Significant cavitation, with increasing propensity at higher test temperatures, occurred in the two alloys but not in pure Zn. A striking feature of the observations in pure Zn and alloy C, as the test temperature was raised, was the formation and subsequent decay of a diamond pattern of uncavitated grain boundaries, a majority of which were preferentially aligned at  $\sim 45^\circ$  to the stress axis. By comparison the changes in the angular distribution of grain boundaries was least marked in alloy A. Cavitation was observed in alloy C to maintain grain boundaries in the  $45^\circ$  orientation. At the test temperature of 150°C alloy C, which was prone to the formation of diamond grain-boundary configuration, developed much larger volume fraction of cavities than alloy A. These results are discussed in terms of the different distribution coefficients of Cu and Al in Zn, the different rates of grain-boundary migration in pure Zn and the two alloys and the differences in the substructural features (cells) formed during high-temperature deformation.

## 1. Introduction

Deformation, recovery and fracture at high temperatures ( $> 0.4 T_m$ ), where  $T_m$  is the melting temperature in K) of polycrystalline metals are characterized by processes associated with the grain boundaries [1]. Among these, few quantitative studies have been made on grain-boundary migration [2] as compared to extensive investigations on grain-boundary sliding [3] and grain-boundary cavitation [4]. Grain-boundary migration is important because of its association with recovery processes, dynamic recrystallization and grain growth and because of the bearing it has upon grain-boundary sliding and cavitation. During high-temperature fatigue and during hot-working extensive migration is observed. A striking feature of migration during high-temperature fatigue is the metallographic observation on plane surfaces of the so-called *diamond* or orthogonal configuration of grain boundaries occurring as a result of their migrating to stable

positions at  $\sim 45^\circ$  to the stress axis [5-10]. This phenomenon has been shown [10] to have a bearing on intergranular cracking during fatigue. The present work is concerned with deformation under creep conditions and observations upon grain-boundary migration, with particular reference to the presence of solutes.

## 2. Experimental procedure

Zn (99.99% pure), Zn-0.14 at. % Cu and Zn-0.16 at. % Al were used. The compositions of the alloys are given in Table I. The distribution coefficient ( $k$ ) is greater than 1 for Cu and equal to 0.25 for Al in Zn and this may be assumed to cause Gibbsian segregation with a depletion of Cu or a build-up of Al atoms at the grain boundaries. This has been shown [11] to give rise to grain-boundary softening due to Cu and grain-boundary hardening due to Al in quenched Zn.

Tensile specimens with 4.5 mm diameter and

TABLE I Compositions of the zinc samples

Alloy	Zn	Cu	Al	Fe	Pb	Cd
Pure zinc	99.99	—	—	0.0009	0.0006	0.00007
Alloy C	99.86	0.14	—	0.0040	0.0009	—
Alloy A	99.84	—	0.16	0.0040	0.0009	0.00007

16.0 mm gauge length were machined from extruded rods. Following machining, the specimens were chemically polished (polishing solution contained 32 g chromic acid and 4 g sodium sulphate in 100 ml of water) to remove the deformed layer and annealed at 250°C for 1 h to yield average grain sizes of 460, 120 and 80  $\mu\text{m}$  in pure Zn and alloys C and A respectively. Slow tensile tests were made at 23°C (0.41  $T_m$ ), 67°C (0.49  $T_m$ ), 100°C (0.54  $T_m$ ) and 150°C (0.61  $T_m$ ) on a modified Hounsfield Tensometer [12] using a nominal strain rate of  $10^{-2} \text{ h}^{-1}$ . Fractured specimens were sectioned longitudinally and chemically polished. The angular distribution of grain boundaries relative to the stress axis in the undeformed and fractured specimens was determined by following a procedure suggested earlier [13]. In order to minimize the errors due to extensive interlinking of cavities in the fractured region, measurements were not made closer than one specimen diameter to the fractured end. More than 200 boundaries in all samples (except in high purity Zn where, owing to coarse grain size, the minimum number was 50 boundaries) were considered. The results are plotted as angular distribution histograms in which per cent relative frequency is shown against angle made with the stress axis. The extent of creep cavitation in the fractured samples was assessed by estimating the per cent volume fraction ( $f$ ) of cavities, using the formula [14]

$$f = \frac{8}{3\pi} \frac{N_L^2}{N_A} \times 100 \quad (1)$$

where  $N_L$  and  $N_A$  are respectively the number of cavities per unit length and unit area. Measurements of  $N_L$  and  $N_A$  were made at  $\times 200$  magnification and the entire area covering the gauge length of the samples was scanned for the purpose.

### 3. Results

Fig. 1 summarizes annealing experiments on these alloys [15]. The presence of solutes is seen to influence the extent of grain growth during annealing. Boundary mobility under purely

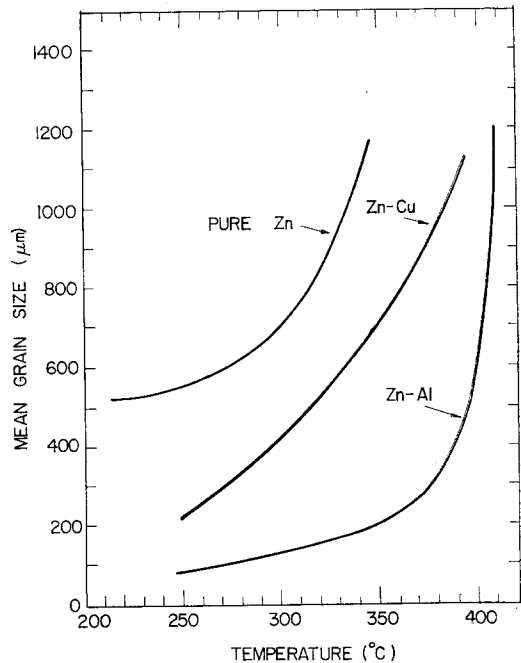


Figure 1 Annealing curves for pure Zn, alloys C and A showing grain growth as a function of temperature after 24 h anneal.

thermal driving conditions appears to be highest in pure Zn, next in alloy C and least in alloy A. Alloy A experiences severe restrictions in grain growth except at temperatures approaching the melting point (419.5°C). During creep, grain-boundary migration occurred most readily in pure Zn, less so in alloy C and was severely restricted in alloy A. Relative amounts of grain-boundary migration during creep deformation are made clear in the angular distribution histograms of apparently uncavitated boundaries plotted in Fig. 2a, b and c. Migration is observed to alter the nearly random distribution of grain boundaries in annealed (untested) samples of pure Zn and alloy C to distributions in which alignment at 45° with respect to the stress axis is preferred (Fig. 2a and b). The peaking of the distribution at  $\sim 45^\circ$  occurs to an increasing

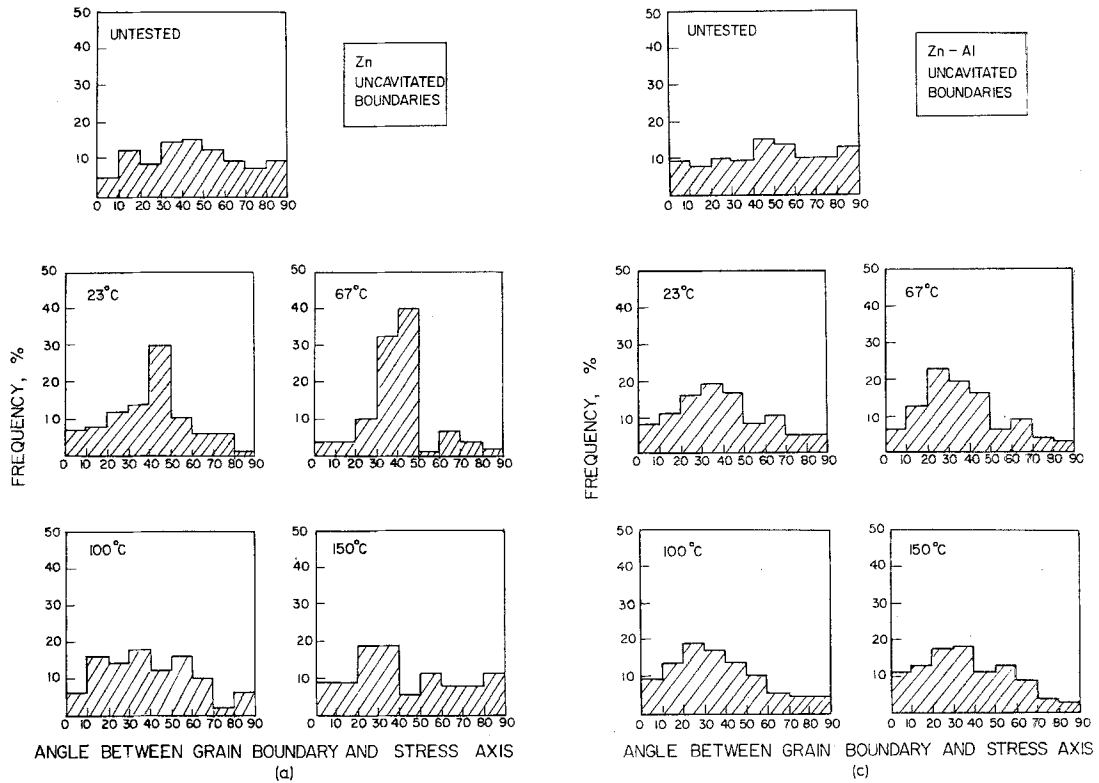


Figure 2 Histograms showing angular distribution of uncavitated grain boundaries with respect to stress axis for specimens untested and fractured in slow tension in the temperature range 23 to 150°C. (a) Pure zinc; (b) alloy C; (c) alloy A.

degree as the temperature of deformation is raised. In high-purity Zn, the maximum 45° alignment occurs at 67°C and in alloy C this takes place at 100°C (Fig. 3).

Boundaries at 45° to the stress axis experience maximum shear stresses. Sliding at such boundaries may induce cavitation on account of the build-up of stress concentrations. Purity once again exerts a marked influence and it is observed that while cavities were generated in alloys C and A from the lowest test temperature (23°C), in the pure Zn sample little cavitation occurred during deformation up to 100°C and a low level of cavitation, with cavities isolated within the grains was observed at 150°C. In Table II are recorded volume fractions of cavities measured in samples fractured at 23, 67, 100 and 150°C. It is important to note that in comparison with alloy A, alloy C cavitated somewhat less at 23 and 67°C, somewhat more at 100°C and markedly more at 150°C.

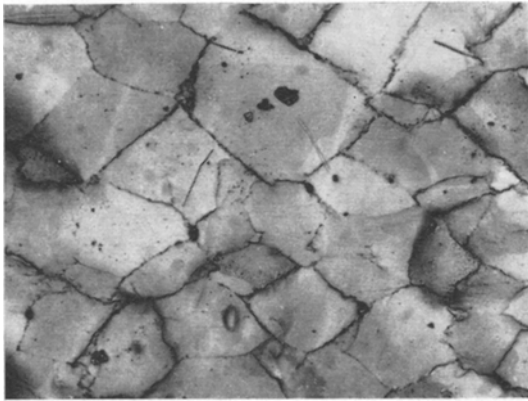


Figure 3 Alloy C tested in slow tension to 20% nominal strain at 100°C showing alignment of grain boundaries at  $\sim 45^\circ$  to the stress axis which is parallel to the long edge of the figure ( $\times 70$ ).

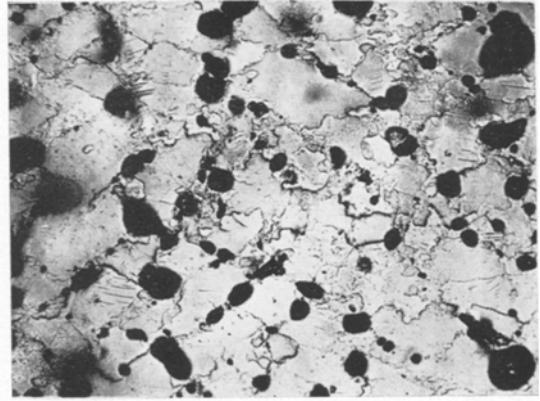


Figure 4 Alloy C fractured in slow tension at 150°C showing cavitated boundaries at  $\sim 45^\circ$  to the stress axis which is parallel to the long edge of the figure. Uncavitated boundaries are seen to migrate to more random orientations ( $\times 55$ ).

TABLE II The effect of test temperature on volume fraction of cavities in fractured samples of pure zinc and alloys A and C

Test temperature (°C)	Volume fraction of cavities (%)		
	Zn	Alloy A	Alloy C
23	Not detected	1.3	0.9
67	Not detected	3.0	2.3
100	Not detected	4.0	4.8
150	0.95	5.0	11.7

In pure Zn, migration continues even after the maximum attainment of  $45^\circ$  alignment ( $67^\circ\text{C}$ ) and the tendency at increasing temperatures of deformation is for the grain boundaries to return to more random configurations. Marked cavitation occurred in alloy C, particularly at higher test temperatures, as pointed out above, and at  $150^\circ\text{C}$  a majority of the boundaries aligned at  $45^\circ$  were cavitated (Fig. 4). While the uncavitated boundaries tend to migrate out of the  $45^\circ$  positions when alloy C is tested at  $150^\circ\text{C}$  (Fig. 2b), the histograms in which the cavitated boundaries are also included show stabilization of the diamond pattern (Fig. 5a).

As against the observations on pure Zn and alloy C noted above, the tendency towards attainment of the diamond grain-boundary configuration is least in alloy A (Fig. 2c). Relatively there is also, in alloy A, no marked difference in the angular distributions of grain boundaries at different test temperatures, with or without the inclusion of cavitated boundaries (Figs. 2c and 5b).

The results contained in the histograms are brought together in Fig. 6 in which is plotted relative frequency of boundaries in the  $30$  to  $60^\circ$  angular range with respect to the stress axis as a function of temperature for all the three materials studied. These results and the others described above may be summarized as follows.

1. A significant diamond-grain configuration due to the alignment of grain boundaries at  $\sim 45^\circ$  relative to the stress axis is observed during high-temperature creep.
2. Maximum alignment of boundaries at  $45^\circ$  occurs during deformation at  $67^\circ\text{C}$  in high purity Zn and at  $100^\circ\text{C}$  in the alloy containing 0.14 at. % Cu (alloy C). The tendency towards attainment of this pattern is least in the Zn alloy containing 0.16 at. % Al (alloy A).
3. Impurities induce cavitation during high-temperature deformation. No significant level of cavitation was observed in high-purity Zn up to deformation at  $100^\circ\text{C}$  and a low level of cavitation occurred at  $150^\circ\text{C}$ , while in alloys C and A cavitation was noticeable even after deformation at  $23^\circ\text{C}$  with increasing levels of occurrence as the test temperature was raised. In samples fractured at  $150^\circ\text{C}$ , the volume fraction of cavities was much larger in alloy C as compared to alloy A.
4. Uncavitated boundaries decay from the diamond pattern in high purity Zn and alloy C to more random distributions at test temperatures above those where the pattern was most prominently formed.
5. Cavitation appears to retain boundaries at  $\sim 45^\circ$  positions, as observed in alloy C.

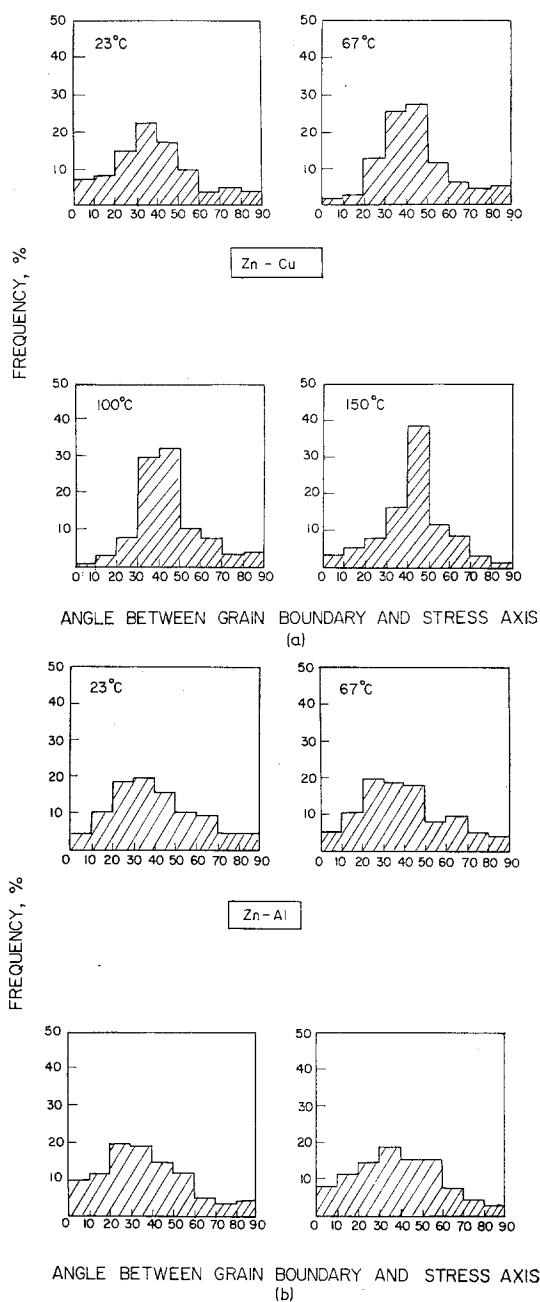


Figure 5 Histograms showing angular distribution of boundaries, including uncavitated as well as cavitated ones, with respect to stress axis for specimens fractured in slow tension in the temperature range 23 to 150°C. (a) Alloy C; (b) alloy A.

#### 4. Discussion of results

The results on grain growth as a function of temperature (Fig. 1) in pure Zn and alloys C and

A can be discussed in relation to the distribution coefficients of Cu ( $k > 1$ ) and Al ( $k < 1$ ) in pure Zn. Solutes with  $k > 1$  are known to experience repulsive interactions [16, 17] and those with  $k < 1$  attractive interactions [11, 18] with grain boundaries in Zn. As shown in Fig. 1, the equilibrium grain size in pure Zn is always largest, suggesting least restraint on boundary mobility. By comparison, grain growth is more restricted in alloy C and, below about 390°C, grain growth is most severely restricted in alloy A. At temperatures above 390°C grain growth becomes very temperature-dependent in alloy A.

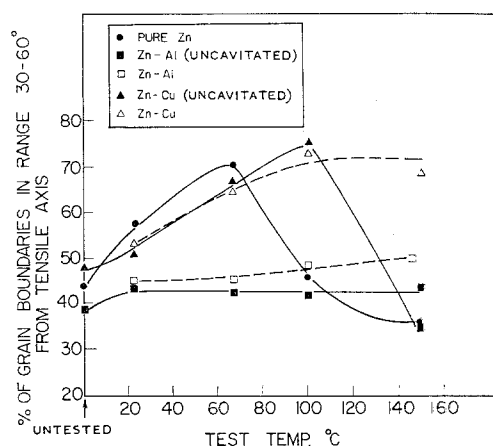


Figure 6 Summary plot of histograms shown in Figs. 2 and 5.

In view of the repulsive interactions that Cu atoms experience, the restraining influence on grain growth due to Cu may be understood in terms of the necessity for Cu atoms to diffuse away from the moving grain boundaries in Zn during annealing. Diffusion across the boundary, necessary during grain growth, is also rendered more difficult in alloy C. Niessen and Winegard [18], who have studied grain growth phenomena in the temperature range 360 to 410°C in similar alloys of Zn, have attributed the high observed activation energies for grain growth in the presence of solutes with  $k > 1$  to an interesting observation that fourfold junctions are stabilized by the collection of solutes because of a leading atmosphere of solutes ahead of the moving grain boundary.

The large decrease in grain growth in alloy A is because Al atoms are adsorbed at the grain boundary and cause a decrease in grain-boundary energy which is the driving force for grain

growth during annealing. Moreover, grain boundary migration would tend to drag solutes ( $k < 1$ ) with it. The concentration maximum is likely to lag behind the migrating boundary and this will result in further accumulation of Al atoms at the boundary. This may be visualized as a self-locking behaviour leading to severe restrictions on grain growth. At temperatures above about 390°C, thermal activity appears to overcome the self-locking phenomenon, rendering grain growth sensitive to temperature. Also, it is important to note that the extent of segregation of Al atoms at grain boundaries is diminished at high temperatures [19] when the activity coefficient of the segregating solute approaches unity [11].

The results shown in Fig. 2a and b appear to constitute the first detailed measurements of angular distribution of grain boundaries during high-temperature creep deformation in which the formation of the diamond pattern of grain boundaries (Fig. 3) is significantly observed. There have been, however, several investigations on high temperature fatigue [5-10] in which such a microstructural development has been noted. Although their primary interest was in high-temperature fatigue, Wigmore and Smith [9] do refer to having observed similar microstructures in Cu tensile-deformed at elevated temperatures.

There have been several suggestions for understanding the phenomenon of diamond-grain boundary configuration in high-temperature fatigue. In polycrystalline Pb fatigued at room temperature ( $0.5 T_m$ ) in which the evolution of a "square" pattern of grain boundaries was observed, Snowden [5], in an attempt to relate the observed grain-boundary reorientation to intragranular deformation, measured the angular distribution of slip traces and found a marked tendency for them to occur at angles near  $\pm 45^\circ$  positions with respect to the stress axis, in agreement with the prediction made by Hedgepath [20] for monotonic deformation. In a later investigation in bicrystals of Pb fatigued at room temperature, Snowden [6] made the important observation that the grain boundaries became serrated by reciprocal migration in the first few per cent of the life, during which the dislocation density increased rapidly. Intense slip striations grew from the corners of serrations and their alignment with the direction of boundary segments suggested their formation by dislocations produced by grain-boundary sliding. Moreover, in the presence of air, cracks were

observed to form as a result of sliding of the serrated boundary.

Wigmore and Smith [9] have suggested a model for the grain-boundary alignment at  $45^\circ$  positions in which the role of grain-boundary sliding is again emphasized. Here they suggest that ahead of boundaries already at  $45^\circ$  positions higher local strain is induced on account of the higher shear stresses acting on the boundaries compared to adjoining boundaries which are not initially at  $45^\circ$  orientation; in the regions ahead of these the local strain will be relatively lower. The defect imbalance is minimized by the movement of grain boundaries which are initially not at  $45^\circ$  positions, towards such orientations. Westwood and Taplin [10] have observed in Fe fatigued at 700°C the formation of sub-boundaries at  $45^\circ$  positions, with grain boundaries aligned parallel to the sub-boundaries. They suggest that some of the intragranular slip arises as a consequence of the requirement for accommodation of sliding displacements at triple junctions; dislocations build up on planes experiencing maximum resolved shear stress and then climb to form low-angle boundaries, associated with which is a surface tension and defect imbalance driving grain boundaries to align themselves parallel to the sub-boundaries.

The following points may be made in regard to the formation of a diamond pattern of grain boundaries in the present work. In a search for the existence of any texture associated with the diamond grain-boundary configuration, an X-ray back-reflection picture (Fig. 7) was taken of alloy C tested at 100°C, in which this configuration was most prominent. No marked variation of diffracted intensity is noticeable around the Debye rings.

Polarized-light microscopy was then carried out on all the three varieties of Zn investigated here, following deformation. Fairly extensive metallographic studies of Zn deformed at high temperatures have been carried out in the past with particular attention paid to the formation of subgrains, also called cells [21-23]. The important finding of the present polarized-light microscopic work is that while pure Zn and alloy C samples revealed cells, very little or no cell formation occurred in alloy A deformed at any of the test temperatures. Cell formation was most prominent in alloy C tested at 100°C (Fig. 8) in which the diamond pattern of grain boundaries was also most prominent. With reference to Fig. 8, it is significant that cell



Figure 7 X-ray back reflection pattern of alloy C fractured in slow tension at 100°C.

boundaries are also aligned at approximately 45° to the stress axis. There is variation from grain to grain in regard to cell formation and the reason is perhaps, as Cahn *et al* [22] point out, that cells occur most readily in those grains in which basal slip is excluded. Among the several sources of driving force suggested for grain-boundary migration during high-temperature creep [2, 24], the one that is relevant to the present discussion is the unbalanced pull exerted on the grain boundary by the subgrains on one side of a grain boundary when these are more numerous than

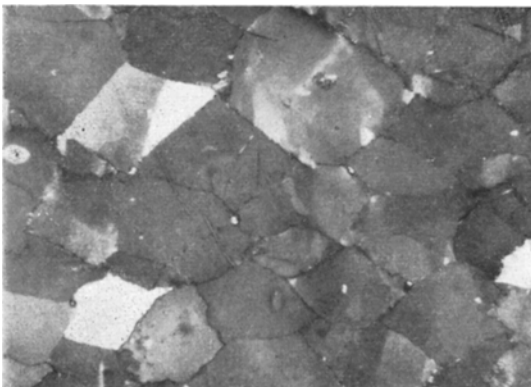


Figure 8 Alloy C pulled in slow tension to 20% nominal strain at 100°C; the same region as in Fig. 3 examined under polarized light shows cell formation. The stress axis is parallel to the long edge of the figure ( $\times 70$ ).

those on the other side [24, 25]. This type of driving force, which could be responsible for the grain boundaries moving up to 45° orientations, is then analogous to the one described above in the model of Wigmore and Smith [9] involving a defect imbalance.

The question, whether or not there does exist a predominant influence of the cell structure on the formation of the diamond grain boundary configuration, needs to be investigated in depth. For the present it is interesting to record that there does seem to be an association between these two events. Besides the fact, mentioned above, that cell formation was most extensive when the diamond pattern of grain boundaries was most prominent, the opposite was also true. At low test temperatures (e.g., 23°C in alloy C) as well as at high-test temperatures (e.g., 150°C in alloy C) when the 45° alignment of uncavitated boundaries was not marked, cell formation was also not prominent. Similarly at high strain-rates, cell formation is known to be inhibited [26]. A sample of alloy C, tested at 100°C using 360 times ( $3.6 \text{ h}^{-1}$ ) the strain-rate ( $10^{-2} \text{ h}^{-1}$ ) at which the diamond pattern had been noted, revealed very few cells, and also no marked tendency for the grain boundaries to align at 45° orientations. In alloy A, as shown by the results on grain growth, grain-boundary migration is severely restricted and this could be an important reason for not observing the kind of reorientation of grain boundaries during deformation as in pure Zn and alloy C. Besides, it is also significant that cell formation was very feeble in alloy A. Greenough *et al* [27] have shown, using Al-2 at. % Ag alloy, that precipitation of  $\text{AgAl}_2$  causes strain fields in the presence of which cell formation during high-temperature deformation is suppressed. Yet another situation of suppression of cell formation is when there exists a misfit strain associated with solute atoms [27, 28]. The absence of extensive cell formation in Zn containing Al could be due to similar causes (the atomic radius of Al atoms is larger than that of Zn atoms by 7.4% and Al atoms segregate to the grain boundaries).

The effect of impurities in inducing cavitation, presented here, has been noted by several investigators in the past [4, 29, 30]. In high-purity metals, continued rapid migration, even after the attainment of the diamond configuration causes stress relaxation and inhibits cavity formation and, when formed, cavities are quickly isolated within the grains, as observed in pure Zn.

The relatively low level of cavitation in alloy C, as compared to alloy A, at test temperatures of 23 and 67°C (Table II) is due to the fact that samples of alloy C in the present investigation had a smaller grain size [31]. The pinning influence of cavitation on grain boundaries, as noted here in alloy C, has also been reported earlier in other metals during high-temperature fatigue [7, 10, 30]. The mechanism suggested by Niessen and Winegard [18] for the stabilization of fourfold junctions during annealing in Zn containing solutes with  $k > 1$  may also have contributed to a delay of the decay of the diamond configuration of grain boundaries and thereby, on account of continued sliding, to the greater extent of cavitation in alloy C (Table II) at higher test temperatures (100 and 150°C). As seen in Figs. 3 and 4, a large number of cavities are observed at the four-fold junctions and along the boundaries aligned at 45° to the stress axis. A preferred site for cavity nucleation has been shown to be the point of intersection of cell and grain boundaries [32]. The existence of these sites in alloy C may also have contributed to the observed greater levels of cavitation in alloy C (Table II).

It is relevant here to refer to the measurements of angular distribution of creep cavities which have been used as a tool in the past to identify the mechanism of growth of cavities during creep deformation. In several of these reports, where grain-boundary sliding is presumed to have caused growth of cavities, prominent peaking around 45° has been observed in the angular-distribution histograms [33-36]. These measurements have borne out the contribution of grain-boundary sliding to cavity growth by demonstrations that at finer grain sizes [33], low strains [33] and at higher strain-rates [37] the 45° orientation of creep cavities is more marked. These investigations have not, however, studied the changes in the orientation of grain boundaries during creep as a result of grain-boundary migration. The present results emphasize the need to investigate this question in all such studies.

Further work is needed to understand the details of inter-relationship between grain-boundary sliding, intragranular deformation, cell formation, grain-boundary migration and cavitation. It is clear, however, that grain-boundary reorientations such as those reported here are important to creep behaviour, to creep strength as well as creep cavitation. As expected, samples with grain boundaries oriented at 45°

with reference to the stress axis have been seen [38, 39] to creep at significantly higher creep rates.

### Acknowledgements

We thank Professor T. R. Anantharaman for encouragement and provision of facilities. Helpful discussions with H. J. Westwood, Kurt H. Roth, V. V. P. Kutumba Rao and Tara Chandra are acknowledged with pleasure. The alloys were kindly supplied by the COMINCO Research Center, Sheridan Park, Canada. Support for this work was given by Banaras Hindu University, and the National Research Council and the Defence Research Board of Canada (Grant 9535-53).

### References

1. D. M. R. TAPLIN, P. RAMA RAO, and V. V. P. K. RAO, Proceedings of Indian Institute of Metals Symposium on Recent Developments in Metallurgical Science and Technology, New Delhi (1972).
2. K. T. AUST, Proceedings of Conference on Interfaces, Ed. R. C. Gifkins (Butterworths, London, 1969) p. 295.
3. R. L. BELL and T. G. LANGDON, *ibid* p. 115.
4. D. M. R. TAPLIN, *Met. Eng. Quart.* **10** (1970) 795.
5. K. V. SNOWDEN, *Phil. Mag.* **6** (1961) 321.
6. *Idem*, *ibid* **14** (1966) 1019.
7. R. P. SKELTON, *Met. Sci. J.* **1** (1967) 140.
8. H. D. WILLIAMS and C. W. CORTI, *ibid* **2** (1968) 28.
9. G. WIGMORE and G. C. SMITH, *ibid* **5** (1971) 58.
10. H. J. WESTWOOD and D. M. R. TAPLIN, *Met. Trans.* **3** (1972) 1959.
11. K. T. AUST, R. E. HANNEMAN, P. NIESSEN, and J. H. WESTBROOK, *Acta Metallurgica*, **16** (1968) 291.
12. V. V. P. KUTUMBA RAO, D. M. R. TAPLIN, and P. RAMA RAO, *Trans. Ind. Inst. Metals* **23** (1970) 61.
13. V. V. P. KUTUMBA RAO and P. RAMA RAO, *Metallography* **5** (1972) 94.
14. R. L. FULLMAN, *Trans. AIME* **197** (1953) 447.
15. K. H. ROTH and D. M. R. TAPLIN, unpublished work.
16. R. A. ORIANI, *Acta Metallurgica* **7** (1959) 62.
17. P. NIESSEN, Ph.D. Thesis, University of Toronto, 1964.
18. P. NIESSEN and W. C. WINEGARD, *J. Inst. Metals* **94** (1966) 31.
19. K. T. AUST and J. W. RUTTER, "Recovery and Recrystallization of Metals" Ed. L. Himmel (Interscience, New York, 1963) p. 131.
20. J. M. HEDGEPTH, National Advisory Committee for Aeronautics (NACA) Technical Note No. 2777.
21. J. A. RAMSEY, *J. Inst. Metals* **80** (1951-52) 167.
22. R. W. CAHN, I. J. BEAR, and R. L. BELL, *ibid* **82** (1953-54) 481.
23. R. C. GIFKINS and J. W. KELLY, *Acta Metallurgica* **1** (1953) 320.



24. N. J. GRANT and A. R. CHAUDHURI, "Creep and Recovery" (ASM, Cleveland, Ohio, 1963) p. 284.
25. P. A. BECK, *Adv. Phys.* **3** (1954) 245.
26. W. A. WOOD, G. R. WILMS, and W. A. RACHINGER, *J. Inst. Metals* **79** (1951) 159.
27. G. B. GREENOUGH, C. M. BATEMAN, and E. M. SMITH, *ibid* **80** (1951-52) 545.
28. R. C. GIFKINS, *ibid* **79** (1951) 233.
29. J. E. HARRIS, *Trans. Met. Soc. AIME* **233** (1965) 1509.
30. J. INTRATER and E. S. MACHLIN, *Acta Metallurgica* **7** (1959) 140.
31. R. G. FLECK, M.A.Sc. Thesis, University of Waterloo, Ontario (1971).
32. A. E. B. PRESLAND and R. I. HUTCHINSON, *J. Inst. Metals* **92** (1963-64) 264.
33. P. W. DAVIES and B. WILSHIRE, *Phil. Mag.* **11** (1965) 189.
34. A. GITTINS and H. D. WILLIAMS, *ibid* **16** (1967) 849.
35. D. M. R. TAPLIN, *ibid* **20** (1969) 1079.
36. A. GITTINS, *Met. Sci. J.* **4** (1970) 186.
37. A. L. WINGROVE and D. M. R. TAPLIN, S.M.D. Report 24 of the University of Waterloo, Ontario (1969).
38. M. KITAGAWA, T. & A.M. Report No. 319 of the Department of Theoretical and Applied Mechanics, University of Illinois, Urbana (1972).
39. H. J. WESTWOOD and D. M. R. TAPLIN, unpublished work.

Received 22 August and accepted 12 September 1972.